IET Power Electronics

Research Article

IET Journals
The Institution of Engineering and Technology

Impact of SiC semiconductors switching transition speed on insulation health state monitoring of traction machines

ISSN 1755-4535
Received on 3rd December 2015
Revised on 17th May 2016
Accepted on 22nd June 2016
doi: 10.1049/iet-pel.2015.0988
www.ietdl.org

Clemens Zoeller[1] ✉, Markus A. Vogelsberger[2], Thomas M. Wolbank[1], Hans Ertl[1]

[1]*Institute of Energy Systems and Electrical Drives, Vienna University of Technology, Gusshausstrasse 27-29, 1040 Vienna, Austria*
[2]*Bombardier Transportation Austria GmbH, Internal Supply Chain (ISC), Hermann Gebauer Straße 5 1220 Vienna, Austria*
✉ *E-mail: clemens.zoeller@tuwien.ac.at*

Abstract: In modern traction propulsion applications, voltage source inverter (VSI) fed traction motors today operate very close to borderline conditions. With new emerging semiconductor technologies, higher inverter switching frequencies will be possible and high inverter dv/dt-rates appear, resulting in transient overvoltages at the machine which increase the stress on the insulation system and lead to insulation degradation. Thus, insulation condition monitoring is getting more and more important to ensure a safe and reliable operation of traction motors in trains and locomotives, trams and so on. This study proposes an online insulation monitoring approach that is able to detect incipient insulation defects by evaluation of the motor transient current response on voltage pulses injected by standard inverter switching. Experimental results of this concept are obtained with tests on a 1.4 MW induction machine for railway application. Additionally, the influence of different dv/dt-rates up to 20 kV/μs on the monitoring performance is verified using a VSI-inverter equipped with SiC semiconductors.

1 Introduction

To achieve safe and efficient traction drive applications for modern railway systems (public and cargo transportation), availability and reliability are key issues. In general, electrical machines are highly reliable and robust. However, the increased electrical stress on the machine's insulation system in case of inverter-fed operation leads to additional insulation strain and ageing. It is common, that insulation breakdown is usually a slowly proceeding process starting with deterioration of the insulation material itself and then leading to severe turn-to-turn, phase-to-ground short circuit (cf. Fig. 1). Hence, the proposed online insulation condition monitoring strategy assists in detecting insulation degradation in an early stage. This provides the possibility for strategic maintenance – react timely on an incipient insulation's defect without the risk of a sudden breakdown.

The main causes for machine breakdown have been analysed in [1–7]. The fast rise times of voltage pulses applied by modern standard switching devices like insulated gate bipolar transistors (IGBTs) and beyond that, by using upcoming wide-bandgap semiconductors [SiC-metal-oxide-semiconductor field effect transistors (MOSFET)/diode combinations] as presented in a later section, result in low switching losses, but ultra-high dv/dt-rates in combination with impedance mismatch (machine against cabling and surge). The fast switching leads to transient overvoltage and thus highest strain for the machine's insulation. The literature clearly states, that the magnitude of the applied voltage and the temperature are the main root causes influencing the insulation status/life time [8–10].

In the first pre-fault stage, the deterioration process of the insulation is usually slowly developing and accelerates rapidly in the final stage, resulting for example in an inter-turn short circuit, which is an actual fault condition. Current practice for insulation condition tests in industry are dissipation factor tan(δ) with tan(δ) tip-up [11], partial discharge [12, 13] and polarisation index or surface insulation resistance test [14]. Principally, most of the tests are applied with the machine partly disassembled from the drive system. Thus, these tests can be referred to as off-line tests, which require by definition a short outage [15–17]. In contrast, on-line tests are applied during operation, although, in some cases the condition of the machine operation is changed to enable a correct diagnose. In [18, 19], the presented on-line techniques require additional signal injection sources, which in turn require additional coupling and decoupling equipment to enable the evaluation of the test signals. These systems or additional components are bulky and mostly undesirable.

Another issue is that remaining life cannot be ascertained. Especially methods that are presented in [20–23] to diagnose insulation problems are better suited for detection of an existing fault than detecting an imminent degradation of turn-to-turn insulation of the stator winding.

The target and key requirements of the proposed on-line insulation monitoring technique is the usage of the already existing current sensors exclusively (e.g. transducers used for machine control) and the online applicability for voltage source inverter (VSI)-fed drives [3, 7]. It has to be noted that the technique is aiming on detection of insulation degradation, i.e. developing fault (deterioration of the insulation prior the actual short circuit) and is based on evaluating the signal information detectable in the transient current response on inverter voltage pulses to detect changes in the machine's insulation system. Thus, a winding condition method is proposed without the need of additional signal injection sources and disassembling of the drive. With the ability to determine the severity of the winding deterioration, the risk of failure can be estimated. In this context, the term 'risk of failure' means that an outage is probably if a transient error occurs. This enables prioritising maintenance, e.g. in a fleet where many drives are in service and neither time nor resources for maintenance of all machines is available.

2 Transient high-frequency behaviour

An inverter-fed drive system can be described in principle by three main components (inverter, cabling and machine), which define a complex impedance system. Its parasitic high-frequency components are mostly defined by the machine insulation system and its actual status. Changes in the machine's insulation system

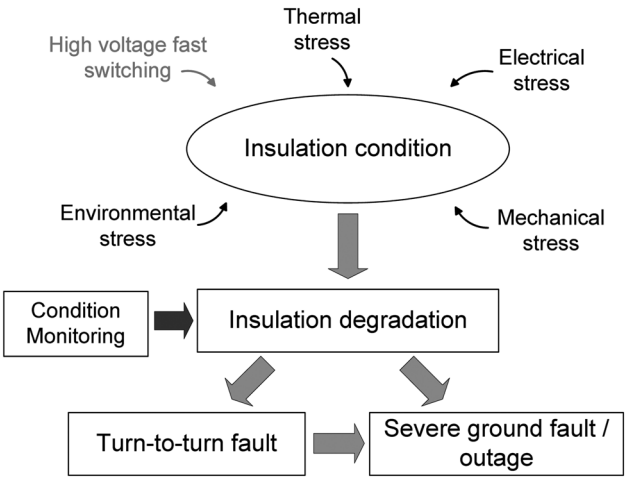

Fig. 1 *Root causes of insulation deterioration and resulting failure*

(e.g. due to insulation degradation or fault) thus results in changes of the insulation capacitances [2] and lead to different voltage ringing and corresponding transient current response (hf-current oscillation). This can be used to analyse the machine's insulation status [3].

The current response stimulated by inverter switching (cf. Figs. 2*a* and *b*) is sampled with sufficient resolution in time, by using an oversampling technique to accurately resolve the included high-frequency components. The current response is recorded using the common built-in current transducers of the inverter (Hall-effect-based closed-loop transducers) with a bandwidth specification of $f_{3\,\mathrm{dB}}$ ~150 kHz. Target and key requirements of the proposed online insulation monitoring technique is the usage of the already existing sensors exclusively. With the simplified assumption that the recorded signal $i(t)$ after a voltage step excitation is a superposition of a linear current rise part, defined by the inductance of the machine and inherent machine asymmetries and a transient part $i_{\mathrm{trans}}(t)$, the trace can be described by the equation: $i(t) \simeq 1/L \int_{-\infty}^{t} u(\tau)\,\mathrm{d}\tau + i_{\mathrm{trans}}(t)$.

The oscillation of $i_{\mathrm{trans}}(t)$ here decays after ~18 µs, afterwards follows the typical inductive behaviour, depending on inherent machine asymmetries, e.g. slotting or saturation, which contains no significant information for the insulation state estimation. As only the hf-oscillation is of interest (containing the insulation state information), the average slope in the current signal has to be eliminated. The blue trace, denoted 'healthy', depicts the transient current response of the machine at the first startup operation of the drive. This curve serves as a fingerprint and is used in a comparison process as reference trace. The green trace, denoted 'degraded insulation', shows the current response of the same machine with emulated insulation deterioration, implemented by a capacitor in parallel to the first coil of phase L1 (in this case insulation aging is emulated only for the first coil), since insulation degradation is linked with a change in the capacitance value of the winding system [24–26]. The characteristics of the deviation in the shape of the first 18 µs are analysed in the frequency domain. After the accurate switching time point has been determined, the time domain data is transformed using a simple rectangular windowing function and the Fourier analysis into the frequency domain.

The spectra of the transient current responses are depicted in Fig. 2*c* for a range up to 1 MHz. The affected frequency range depends on the size of the machine and position of the fault capacitor. Previous investigations in [4] on the test machine showed that the highest-frequency component of interest for the estimation of the insulation state is up to 1 MHz. On the basis of the root mean square deviation between the 'healthy' and 'degraded' trace for every equidistant frequency point within a defined frequency range, an indicator is calculated to assess the severity of the insulation degradation. On the basis of the trend of the indicators over time, insulation deterioration can be concluded and further maintenance steps can be introduced. Regarding comparative analyses to estimate a deviation, it is of vital importance that the measurements achieve a high degree of reproducibility. The enlarged subfigure of Fig. 2*c* shows the standard deviation $\pm\sigma$ (solid blue and red area) of the spectral components of totally 50 measurements. As can be seen, the variance of the data points in the spectrum is very low resulting in a high reproducibility. The used current sensors are Hall-effect-based closed-loop transducers. The bandwidth specification with ($f_{3\,\mathrm{dB}}$ ~150 kHz), indicate the range of low level sine-wave frequencies that can be reproduced with a specified reduction in signal amplitude, typically −1 or −3 dB. However, due to the special construction of the sensor with its Hall-generator and the secondary coil acting as compensation coil, the bandwidth is significantly extended and the response time of the sensor is improved. At lower frequencies, the transducer operates using the Hall generator. At higher frequencies, however the secondary coil operates like a current transformer significantly extending the bandwidth and reducing the response time of the transducer. As the frequency range of interest is outside of this low level sine-wave specification, investigations and support from the current transducer manufacturer showed that frequency response up to 1 MHz is reproducible.

A detailed description of the insulation state indicator (ISI) calculation is given in the next section.

3 Insulation state indicator

To achieve a diagnose strategy, it is important to perform measurements on a healthy machine to determine the original insulation state. This serves as a reference and is compared with later measurements in operation (condition measurement) to assess the machine's actual insulation condition

$$\mathrm{ISI}_{p,k} = \mathrm{RMSD}_{p,k}(x_1, x_2) = \frac{\sqrt{\sum_{g=n_{\mathrm{low}}}^{n_{\mathrm{high}}} \left(|Y_{\mathrm{ref},p}(g)| - |Y_{\mathrm{con},p,k}(g)|\right)^2}}{n_{\mathrm{high}} - n_{\mathrm{low}}} \quad (1)$$

$$\mathrm{ISI}_p = \frac{\sum_{k=1}^{m} \mathrm{ISI}_{p,k}}{m} \quad (2)$$

Further, an ISI for the assessment of the insulation condition for each individual phase will be introduced. It is based on comparison of the amplitude spectra for the different states by applying the root mean square deviation (RMSD) as comparative value (1). The Fourier components Y_{ref}, Y_{con} represent the reference and later condition assessment, respectively. The index p defines the investigation phases (L1, L2, L3) and m indices the number of measurement repetitions. The variable $n_{\mathrm{high,low}}$ represents the analysis frequency range defined by sampling frequency and fast Fourier transform (FFT)-window length. In this work, the observation range for the transient current part was set to the first 30 µs after the switching transition. This enables the calculation and subtraction of the accurate current slope to prevent any influences through slotting. The acquired data points (3600) in the time domain, resulting by a sampling frequency of $f_{\mathrm{s}} = 120$ MS/s, are transferred by the FFT-algorithm with a rectangular window function into the frequency domain.

It should be noted that the ISI magnitude correlates with the severity of insulation degradation, and is hence suited to act as the final monitoring value. To detect the spatial location of the insulation degradation, by linear combination of the previous calculated ISI-phase values (2) a spatial ISI (SISI) can be defined (3). Thereby changes of the high-frequency behavior due to temperature variation are eliminated as these would lead to zero-

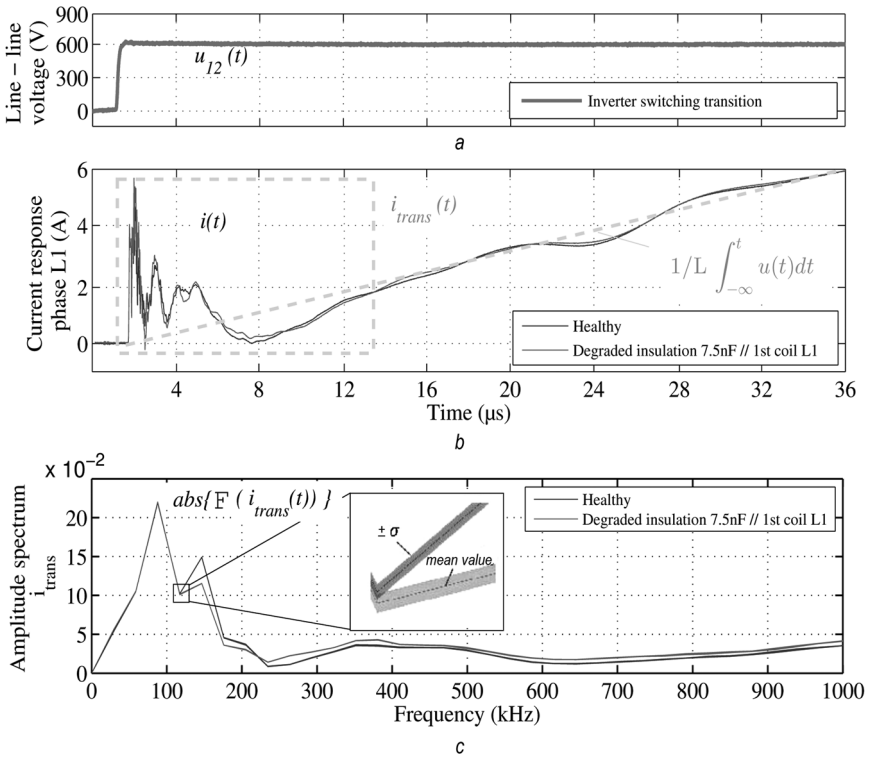

Fig. 2 *Sampled current response stimulated by inverter switching*

a Inverter switching transition (10 kV/μs)
b Transient phase current response blue: healthy machine; green: degraded winding insulation
c Spectra of the transient current responses

sequence components

$$\mathrm{SISI} = \mathrm{ISI}_{L1} + \mathrm{ISI}_{L2} \cdot \mathrm{e}^{\mathrm{j}(2\pi/3)} + \mathrm{ISI}_{L3} \cdot \mathrm{e}^{\mathrm{j}(4\pi/3)} \tag{3}$$

In [3, 7, 24], a detailed description of the fundamentals, theory as well as mathematic calculation of the proposed condition monitoring technique and the ISI are given.

In the next section, the experimental setup is described.

4 Experimental setup

The purpose of this paper is to identify the sensitivity of the proposed online insulation condition monitoring method on different motor-converter systems. Especially, it has to be verified whether the converter dv/dt-rate shows an impact to ISI value. Furthermore, the applicability of the proposed monitoring technique for a three-phase ac railway motor under the constraint that the motor is fed by a converter with very high dv/dt-rate (e.g. caused by an SiC-VSI) will be tested. The experimental investigations are carried out on a high power traction machine (4-pole 1.4 MW squirrel-cage asynchronous machine (ASM) with fibre-insulation wires), cf. Fig. 3.

As aforementioned in the introduction, each step input introduced by the PWM waveform into a power drive system, with the inverter-cabling-machine arrangement depicted in Fig. 3, elicits a specific system response. When subjected to a high dv/dt voltage rise, all parasitic components interact with each other and produce ringing. The figure illustrates the measurement procedure by applying a voltage step with the inverter from lower short circuit to high DC-link voltage in phase L1. The procedure is repeated for every phase separately. The measurements were conducted at stand still without magnetisation of the machine and could be implemented as a startup routine prior to operation of the drive. The voltage step excitation in the power drive system elicits a response in the system influenced by the parameters of each element. The cabling system is modelled by per unit length inductance L'_{Cable} and resistance R'_{Cable}. Furthermore, phase-to-phase and phase-to-ground parasitic capacitances ($C_{\mathrm{Ph–Ph}}$, $C_{\mathrm{Ph–Gnd}}$) are considered, which substantially influence the behaviour of the system at higher frequencies. For the motor, the basic parameters are its stator resistance R_{S} and the stator inductance L_{S}. In addition to parasitic winding capacitances, i.e. $C_{\mathrm{Ph–Gnd}}$, $C_{\mathrm{Ph–Ph}}$ and $C_{\mathrm{Turn–Turn}}$ are included which largely influence the high-frequency behaviour and consequently the transient overvoltages at the machine. To perform the alteration of the machine's high-frequency behaviour the test machine is equipped tapped windings, this enables the possibility to insert additional capacitors to change the machine's hf-characteristic, which act as emulated insulation degradation without destruction [3].

For the inverter, in particular its capacitive coupling $C_{\mathrm{Inv–Gnd}}$ to ground is considered. For the analyses in this work, the external gate resistance in the gate drive unit (GDU) can be changed for defining the on- and off-switching times. A higher gate resistance value reduces the charge and discharge current to or from the gate, resulting in lower dv/dt-rates of the output voltage. On contrary, a low resistance value gives fast switching operation and reduces also the switching losses. However, due to the resulting high di/dt values of the main current part, overvoltage peaks may occur depending on the used load.

The ability to vary the output voltage steepness by adjusting the gate resistor makes available to analyse the sensitivity of the proposed method regarding inverter dv/dt-rates.

For testing the proposed drive monitoring, a three-phase pulse generator has been designed and implemented featuring test pulse signals at dv/dt-rates up to 25 kV/μs for amplitudes of up to 800 V (Figs. 4*a* and *b*).

The setup consists of two boards, the power board containing all main power components such as semiconductors, dc-link capacitors and so on, and the control board which basically includes the GDU and over-current protection. Three individual half-bridge stages of two discrete SiC-MOSFETs with additional external free-wheeling

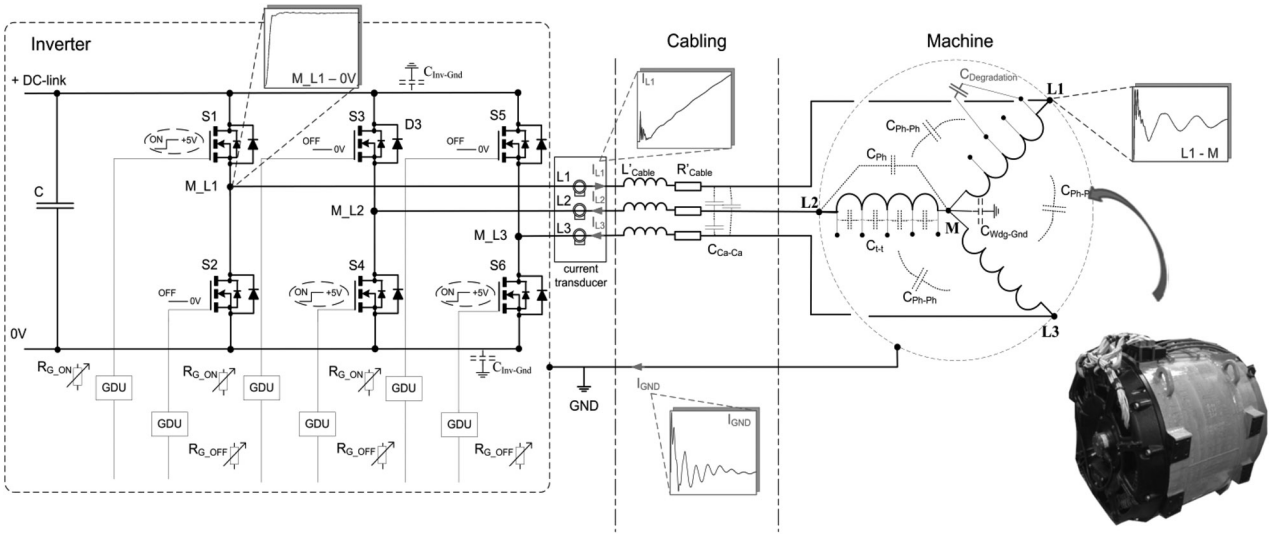

Fig. 3 *Scheme of the test stand with inverter, cabling and machine. Additional capacitor $C_{Degradation}$ inserted in parallel to the phase winding (schematically drawing) 1.4 MW induction machine (winding taps accessible at terminal connection block)*

SiC-diodes enable the excitation of each phase separately. All semiconductor devices are grouped on a power printed circuit board containing electrolytic DC link capacitors which is characterised by an ultra-low-inductive bi-planar power plane routing. The MOSFETs are controlled by a fully isolated bipolar gate drive stage using standard optocouplers with additional dv/dt improving circuitry. Furthermore, an extension to pulses of 1200 V amplitude is planned.

5 Analysis results

In this section, investigations on the proposed online insulation condition monitoring method and the applicability to inverter fed AC machines with different highly increased dv/dt-rates of the converter output voltage are conducted. As the proposed monitoring method is implemented as a comparative method, it is of vital importance that the detected changes in the frequency range between the initial healthy machine and the same machine with aged insulation system are only due to the winding insulation degradation affects. However, ageing also occurs in the power semiconductors and the effects are analysed in different studies [27–29]. Ageing of the semiconductors in this work is emulated by a deviation of the voltage rise time (dv/dt) from an initial configuration. Due to a small change of the gate resistance in the GDU from the initial value of 42 Ω (dv/dt ∼10 kV/µs), up to 49 and 68 Ω a clear deviation of the rate of voltage rise is applied. The voltage rise with the different gate resistances measured at point M_L1 (cf. Fig. 3) with respect to 0 V potential are shown in Fig. 5*a*. The measured voltage at point L1, showing the voltage at the machine terminal of L1 with respect to starpoint M is depicted in Fig. 5*b*. The effect is still visible and the excitation of the system has changed.

The propagated voltage wave applied by the inverter with different dv/dt-rates and the resulting spectra of the transient current responses for different machine states are depicted in Figs. 6*a* and *b*.

The left-hand side of Fig. 6*a* shows the spectrum for the healthy machine and in case of the same machine with emulated insulation degradation, with the inverter configuration $R_G = 42\ \Omega$. The right-hand side of Fig. 6*b* shows the same machine states in case of a gate resistance $R_G = 68\ \Omega$.

The deviation between the machine states within one inverter configuration (e.g. $R_G = 42\ \Omega$) is clearly observable. With the comparison of the healthy machine scenario of a measurement with 42 Ω with the emulated insulation degradation case (3, 7.5 and 15 nF//first coil) with a gate resistance of 68 Ω (see Table 1, third row), a change of the voltage rise due to ageing of the semiconductor is considered and the influence on the proposed method is analysed. In the following Table 1, the indicator values are calculated and show the monotonic increasing behaviour. The estimated phase-to-ground capacitance for the 1.4 MW test machine is about 21 nF. Thus, the emulation of the insulation degradation with a ΔC of 1.5 nF corresponds to a change of 7% of the total phase capacitance.

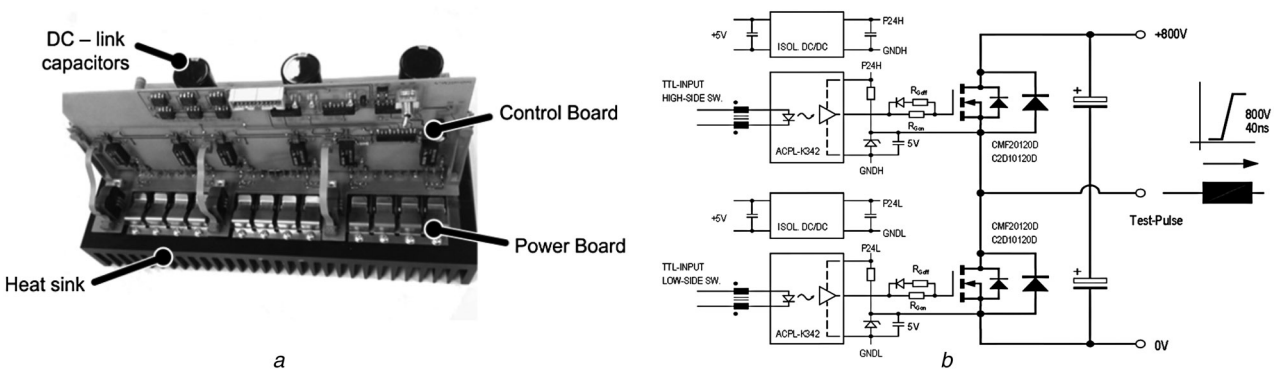

Fig. 4 *Testing the proposed drive monitoring*

a Three-phase test pulse generator; SiC-MOSFET half-bridge stages with dedicated external SiC-free-wheeling diodes
b Circuit diagram of designed and implemented test pulse generator in SiC technology

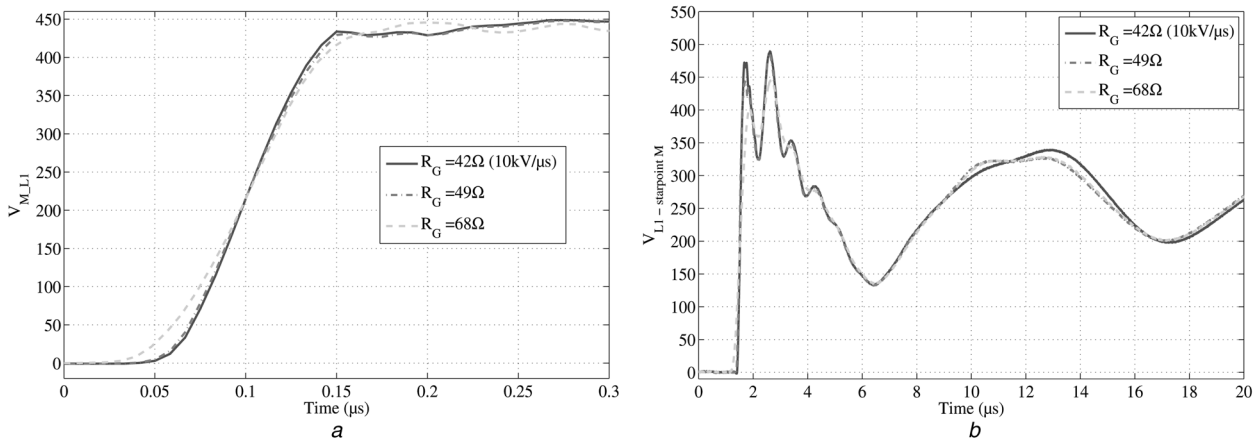

Fig. 5 *Voltage rise with the different gate resistances measured at*

a Voltage M_L1 with respect to 0 V in case of different gate resistor values
b Machine terminal voltage L1 with respect to starpoint M in case of different gate resistor values

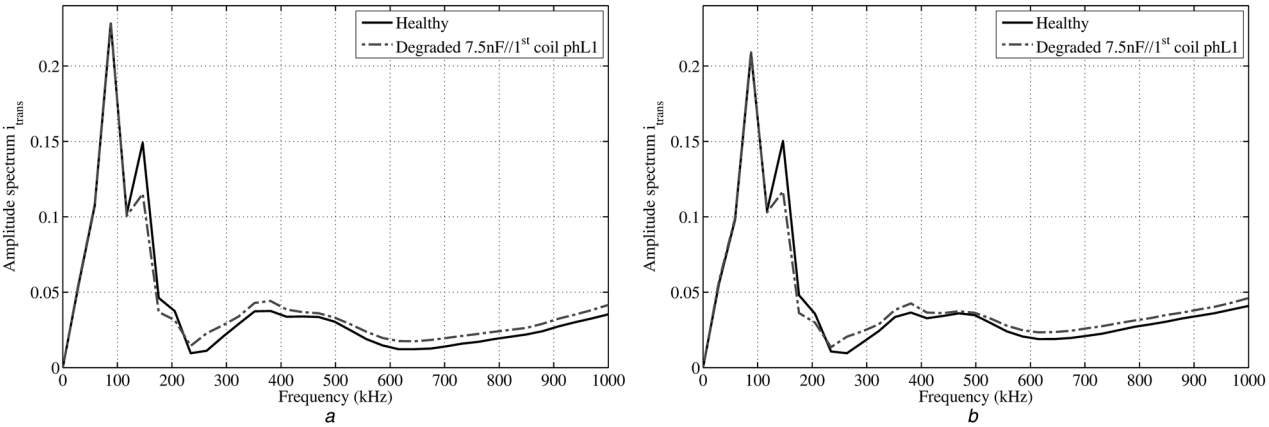

Fig. 6 *Propagated voltage wave applied by the inverter and the resulting spectra of the transient current responses for different machine states*

a Reference amplitude spectrum (healthy: blue), and in case of degraded machine insulation (green); gate resistor 42 Ω; voltage rate: 10 kV/µs
b Reference amplitude spectrum (healthy: red), and in case of degraded machine insulation (cyan); gate resistor 68 Ω

Investigations from the authors in [4] with accelerated thermal ageing of insulation systems in a stator slot model show that the capacitance value of the specimens typically change up to 20% of the initial value. Thus, the emulated insulation degradation scenarios with capacitor values from 1.5 to 15 nF seems to be a realistic value. To improve the accuracy, it is important that the test bench is complying with the EMC specification. The Hall-effect-based closed-loop transducers are placed in a shielded sensor box and are connected with shielded cables to prevent disturbing influences. The measurement and signal processing is carried out with a real-time system combined with a field programmable gate array with a fast sampling analog digital converter (ADC) (120 MS/s) and 16 bit resolution. Regarding the several times lower sampling rate of the typically available ADC units in a drive system, the frequency resolution is restricted by the Nyquist criterion. However, the frequency range can be enhanced by use of simple sampling techniques, e.g. equivalent time-sampling, also often named repetitive sampling. Investigations showed that satisfying results are achieved with a sampling rate of ten times higher than the interesting frequency. Instead of gathering all samples for a waveform with one trigger event, the system acquires the data with several trigger events over multiple measurements shifted by a multiple of the reciprocal of the required sampling rate. Several voltage steps and corresponding current responses then form one response of the system. Concerning the bit resolution, 10 bit are sufficient to achieve adequate accuracy. This resolution is easily met in modern drive systems.

The nominal current range for the utilised current transducers is up to 200 A. The output of the transducer is a secondary current signal, related to the input current scaled by the turns ratio ($N_P/N_S = 1/2000$). For a given turns ratio and maximum expected input current, the burden resistance was selected to adapt the output signal to the maximum input range of the data acquisition system (−1 to +1 V).

Concerning the tests scenarios of emulated insulation degradation by insertion of a capacitor from 330 pF to 15 nF capacitor in parallel

Table 1 Results of the indicators for machine scenarios

Machine state	Healthy	1.5 nF//First coil phase L1	3 nF//First coil phase L1	7.5 nF//First coil phase L1	15 nF//First coil phase L1
ISI value (42 Ω)	0.26×10^{-3}	2.03×10^{-3}	3.66×10^{-3}	8.51×10^{-3}	16.42×10^{-3}
ISI value (68 Ω)	0.27×10^{-3}	1.99×10^{-3}	3.73×10^{-3}	8.4710^{-3}	16.4×10^{-3}
ISI value (42 Ω (*)/68 Ω (**))	0.26×10^{-3}	2.03×10^{-3}	3.89×10^{-3} (**)	8.48×10^{-3} (**)	17.01×10^{-3} (**)

*Rg = 42 Ω
**Rg = 68 Ω

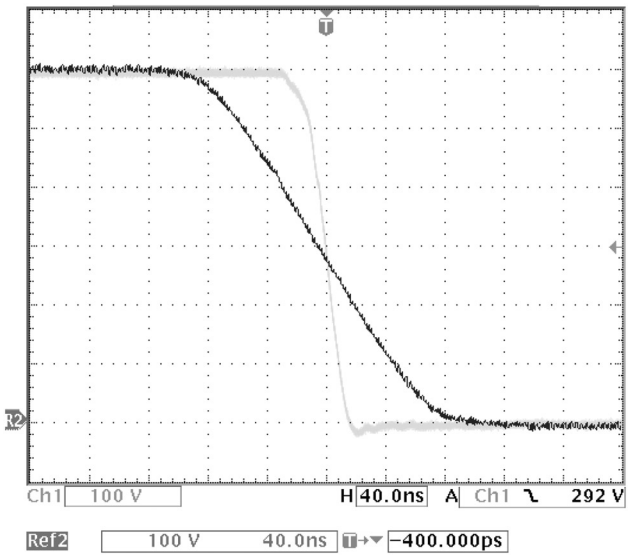

Fig. 7 *Inverter switching falling edge transition (amplitude 600 V) with different dv/dt-rates. (yellow: 20 kV/µs; black: 3 kV/µs)*

to full phase winding and phase-to-phase respectively, and different dv/dt-rates up to 20 kV/µs (Fig. 7), the test results are depicted in Figs. 7–10.

As clearly visible from the amplitude spectra, the dominant frequency band in case of a modified hf-behaviour (insulation status) is changed according the proposed forecast model. Further, the less impact of the voltage rate (dv/dt) to the equidistant values of the amplitude can be read out by comparison of Figs. 6*a* and *b*. Fig. 8 depicts the calculated SISI in the Gaussian plane for different scenarios.

In Fig. 8 it can be seen, that SISI points in the direction of phase L1 as the change of the machine's high frequency has been carried out there (to emulate an insulation degradation). Hence, the phase location of the alteration can be clearly identified. In addition, the distance between origin of the plane and the locus of the SISI-pointer represents the severity of the insulation deterioration.

The degradation of the insulation material usually starts with deterioration of the turn–turn insulation and in the end leading to severe faults affecting coils or the whole phase with final phase to ground faults. Until the complete breakdown of the insulation it is a slowly developing process. This enables to observe a change over a longer period of time.

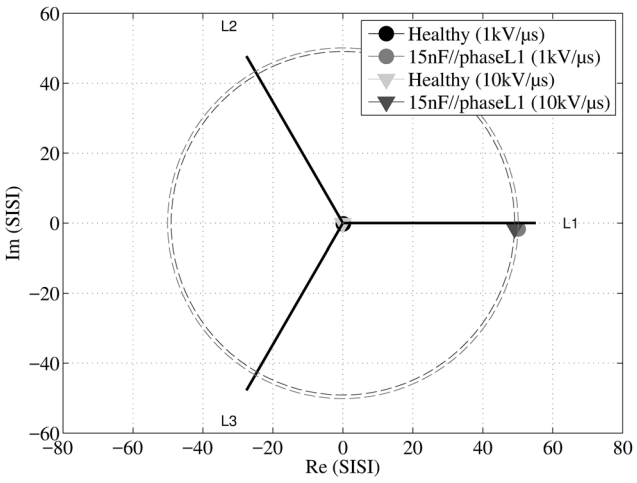

Fig. 8 *SISI for different investigation conditions (healthy machine and condition assessment at different dv/dt-rates)*

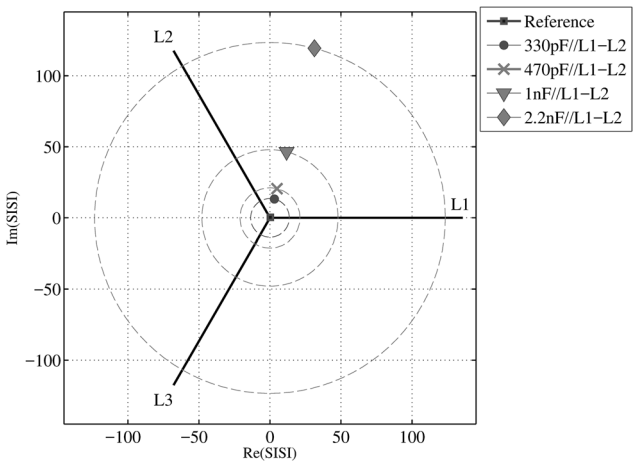

Fig. 9 *SISI for different machine winding insulation conditions and dv/dt-rate of 20 kV/µs (increasing insulation degradation)*

To emulate an imminent degradation of the insulation of the stator winding, the capacitors with 330 pF–2.2 nF are placed separately parallel to phases L1 and L2 (variation of $C_{\mathrm{Ph-Ph}}$), depicted as in Fig. 9. All measurements are based on a converter dv/dt-rate of 20 kV/µs.

As can be seen, all indicators in the Gaussian plane are located and assigned in direction between phases L1 and L2. The indicators show monotonic increasing tendency and the alteration of the capacitors can be clearly identified with increasing capacitor values. In Fig. 10, the single indicators of phase L1 in which insulation degradation occurs if applying (1) and (2) are depicted. Regarding the detection of a fault the measurement taken at initial drive operation (reference measurement) is repeated on the healthy insulation state and due to measurement noise, deviations in the spectra add up to a non-zero value of the indicator. All indicators are scaled to this value and an indicator higher than 1, which is denoted with 'healthy' in Fig. 10, indicates a deterioration of the insulation state.

The measured winding to ground capacitance of the 1.4 MW test machine is about 63 nF (21 nF per phase). With an expected capacitance change of about 20% of the initial value, according to the studies of different authors, e.g. [2, 4], the selected values reflect a realistic change.

It can thus be stated and concluded that the proposed online insulation condition monitoring method is well working and applicable to inverter fed AC machines with different highly

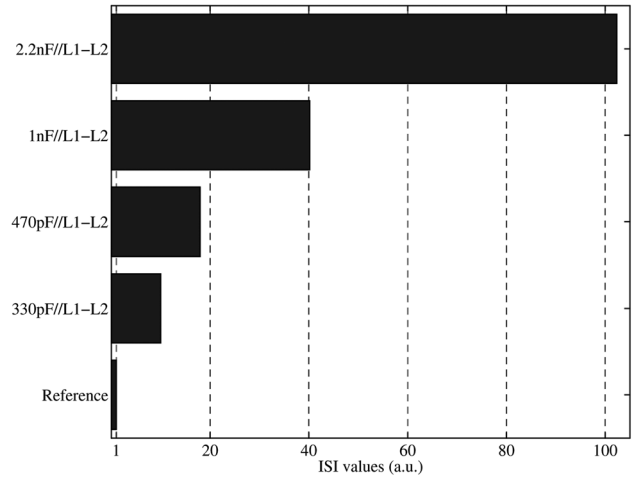

Fig. 10 *ISI of phase L1 for different machine winding insulation conditions and dv/dt-rate of 20 kV/µs (increasing insulation degradation)*

increased dv/dt-rates of the converter output voltage. Different approaches regarding the condition monitoring are described in [15, 16, 19] and can be compared with the proposed method. On the basis of a comparative method and the focus on the high degree of reproducibility of the measurements for the machine states, the deviation between the machine state at initial operation of the drive (reference) and later actual machine state give evidence about the insulation state, which enables to improve maintenance costs and avoid unscheduled downtimes.

6 Conclusions

An insulation monitoring method to detect insulation degradation of three phase ac machines based on the information of the inverter current sensors has been presented. An inverter switching transition is applied to the machine and the resulting phase current responses are analysed. The high-frequency ringing of the current response is important for the insulation state evaluation. These transients are mainly influenced by the drive's parasitic capacitance and insulation degradation is always linked with a change of this capacitance that is considered as the dominant parameter for the estimation of the insulation health state. On the basis of the deviation analysed in the frequency domain in comparison to a reference measurement gained at the first startup of the drive and later in-service measurements, information about the insulation ageing condition is obtained. Laboratory measurements are performed on a 1.4 MW induction machine with winding taps accessible at terminal connection block. The tested emulated insulation degradation scenarios are well detectable and show a monotonic increasing tendency for increasing winding capacitance values. It can thus be stated and concluded, that the proposed online insulation condition monitoring method is well working and applicable to inverter fed AC machines. Different dv/dt-rates of the output voltage of modern drive converters virtually do not influence the monitoring results.

7 Acknowledgments

The work to this investigation was supported and funded by the Austrian Research Promotion Agency (FFG) under project number 838478. The authors thank Bombardier Transportation Mr. D. Baro (GSC/PPC-Drives Global Engineering Head) and Mr. M. Bazant Product Development GSC/PPC Drives for Product-Development Funding, feedback and the great support. Thanks also goes to the LEM-Company (especially Mr. W. Teppan), the National Instruments Austria (Mr. G. Stefan). Special thanks go to the Cree-company (Mr. Das and Mr. Esquivel) for the cooperation and the support.

8 References

1 IEEE Committee Report: 'Report of large motor reliability survey of industrial and commercial installation', *IEEE Trans. Ind. Appl.*, 1985, **21**, pp. 853–864
2 Farahani, M., Gockenbach, E., Borsi, H., *et al.*: 'Behavior of machine insulation systems subjected to accelerated thermal aging test', *IEEE Trans. Dielectr. Electr. Insul.*, 2010, **17**, (5), pp. 1364–1372
3 Nussbaumer, P., Wolbank, T.M., Vogelsberger, M.A.: 'Separation of disturbing influences on induction machine's high-frequency behavior to ensure accurate insulation condition monitoring'. Twenty-Eighth Annual IEEE Applied Power Electronics Conf. and Exposition (APEC), 2013, pp. 1158–1163
4 Zoeller, C., Vogelsberger, M.A., Fasching, R., *et al.*: 'Evaluation and current-response based identification of insulation degradation for high utilized electrical machines in railway application'. IEEE Int. Symp. on Diagnostics for Electrical Machines, Power Electronics and Drives (SDEMPED), 1–4 September 2015, pp. 266–272
5 Yang, D.J., Cho, J., Lee, S.B., *et al.*: 'An advanced stator winding insulation quality assessment technique for inverter-fed machines', *IEEE Trans. Ind. Appl.*, 2008, **44**, (2), pp. 555–564
6 Kaufhold, M., Aninger, H., Berth, M., *et al.*: 'Electrical stress and failure mechanism of the winding insulation in PWM-inverter-fed low-voltage induction motors', *IEEE Trans. Ind. Electron.*, 2000, **47**, (2), pp. 396–402
7 Nussbaumer, P., Vogelsberger, M.A., Wolbank, T.M.: 'Exploitation of induction machine's high-frequency behavior for online insulation monitoring'. IEEE Int. Symp. on Diagnostics for Electric Machines, Power Electronics and Drives (SDEMPED), 2013, pp. 525–531
8 Florkowska, B., Florkowski, M., Roehrich, J., *et al.*: 'The influence of PWM stresses on degradation processes in electrical insulation systems'. Annual Report Conf. on Electrical Insulation and Dielectric Phenomena (CEIDP), West Lafayette, IN, 2010, pp. 1–4
9 Dakin, T.W.: 'Electrical insulation deterioration treated as a chemical rate phenomenon', *Trans. Am. Inst. Electr. Eng.*, 1948, **67**, (1), pp. 113–122
10 Zhang, P., Du, Y., Habetler, T.G., *et al.*: 'A survey of condition monitoring and protection methods for medium-voltage induction motors', *IEEE Trans. Ind. Appl.*, 2011, **47**, (1), pp. 34–46
11 IEEE: 'Recommended practice for measurement of power factor tip-up of electric machinery stator coil insulation'. IEEE Std 286-2000, 2001, pp. i,29
12 Ahola, J., Särkimäki, V., Muetze, A., *et al.*: 'Radio-frequency-based detection of electrical discharge machining bearing currents', *IET Electr. Power Appl.*, 2011, **5**, (4), pp. 386–392
13 Ait-Amar, S., Roger, D.: 'Prospective method for partial discharge detection in large AC machines using magnetic sensors in low electric field zones'. IET Int. Conf. on Computation in Electromagnetics (CEM 2011), 2011, vol. 5, no. 4, pp. 386–392
14 IEEE: 'Recommended practice for testing insulation resistance of electric machinery'. IEEE Std 43-2013, 6 March 2014, pp. 1–75
15 Stone, G.C., Boulter, E.E., Culbert, I., *et al.*: 'Electrical insulation for rotating machines' (IEEE Press, Piscataway, NJ, USA, 2004)
16 Toliyat, H.A., Nandi, S., Choi, S., *et al.*: 'Electric machines: modeling, condition monitoring, and fault diagnosis' (CRC Press, Boca Raton, FL, USA, 2012)
17 Perisse, F., Mercier, D., Lefevre, E., *et al.*: 'Robust diagnostics of stator insulation based on high frequency resonances measurements', *IEEE Trans. Dielectr. Electr. Insul.*, 2009, **16**, (5), pp. 1496–1502
18 Tallam, R.M., Habetler, T.G., Harley, R.G.: 'Stator winding turn-fault detection for closed-loop induction motor drives'. IEEE Industry Applications Conf. (37th IAS Annual Meeting), Pittsburgh, PA, USA, 2002, vol. 3, pp. 1553–1557
19 Neti, P., Grubic, S.: 'Online broadband insulation spectroscopy of induction machines using signal injection'. IEEE Energy Conversion Congress and Exposition (ECCE), 14–18 September 2014, pp. 630–637
20 Ghanbari, T.: 'Autocorrelation function-based technique for stator turn-*fault* detection of induction motor', *IET Sci. Meas. Technol.*, 2016, **10**, (2), pp. 100–110
21 Ramírez-Niño, J., Pascacio, A., Mijarez, R., *et al.*: 'On-line fault monitoring system for hydroelectric generators based on spectrum analysis of the neutral current', *IET Gener. Transm. Distrib.*, 2015, **9**, (16), pp. 2509–2516
22 Arumugam, P., Tahar, H., Gerada, C.: 'Turn–turn short circuit fault management in permanent magnet machines', *IET Electr. Power Appl.*, 2015, **9**, (9), pp. 634–641
23 Van der Geest, M., Polinder, H., Ferreira, J.A.: 'Short-circuit *faults* in high-speed PM *machines* with parallel strands and coils'. IET Int. Conf. on Power Electronics, Machines and Drives (PEMD), 2014, pp. 0435–0435
24 Nussbaumer, P., Wolbank, T.M., Vogelsberger, M.A.: 'Sensitivity analysis of insulation state indicator in dependence of sampling rate and bit resolution to define hardware requirements'. IEEE Int. Conf. on Industrial Technology (ICIT), 25–28 February 2013, pp. 392–397
25 Farahani, M., Borsi, H., Gockenbach, E.: 'Study of capacitance and dissipation factor tip-up to evaluate the condition of insulating systems for high voltage rotating machines', *Electr. Eng.*, 2007, **89**, (4), pp. 263–270
26 Perisse, F., Werynski, P., Roger, D.: 'A new method for AC machine turn insulation diagnostic based on high frequency resonances', *IEEE Trans. Dielectr. Electr. Insul.*, 2007, **14**, (5), pp. 1308–1315
27 Brown, D.W., Abbas, M., Ginart, A., *et al.*: 'Turn-off time as an early indicator of insulated gate bipolar transistor latch-up', *IEEE Trans. Power Electron.*, 2012, **27**, (2), pp. 479–489
28 Somos, L.: 'Power semiconductors empirical diagrams expressing life as a function of temperature excursion', *IEEE Trans. Magn.*, 1993, **29**, (1), pp. 517–522
29 Ginart, A.E., Brown, D.W., Kalgren, P.W., *et al.*: 'Online ringing characterization as a diagnostic technique for IGBTs in power drives', *IEEE Trans. Instrum. Meas.*, 2009, **58**, (7), pp. 2290–2299